Article

Cell Reports

miRNA-Mediated KHSRP Silencing Rewires Distinct Post-transcriptional Programs during TGF-β-Induced Epithelial-to-Mesenchymal Transition

Graphical Abstract

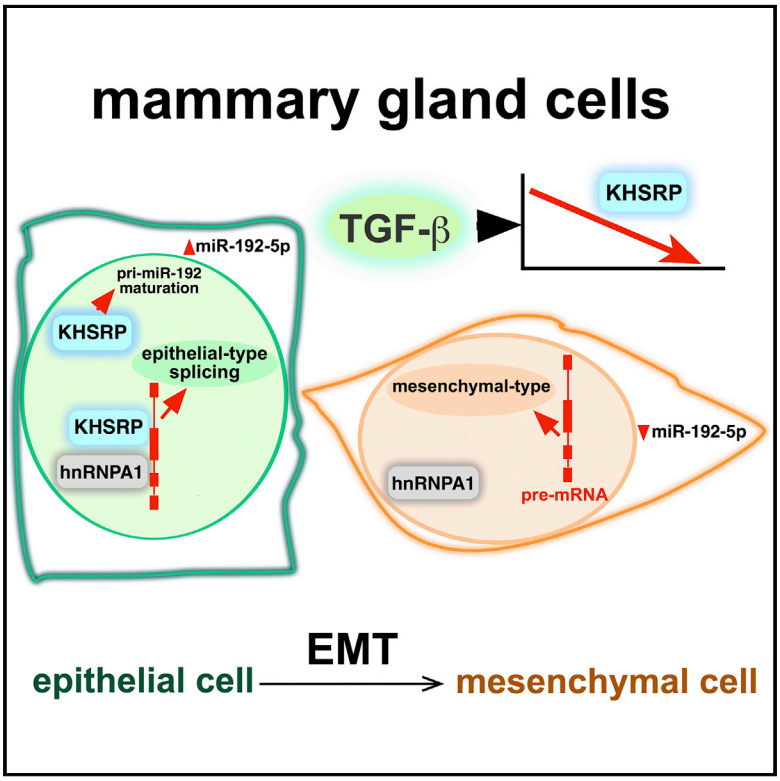

Authors

Margherita Puppo, Gabriele Bucci, Martina Rossi, ..., Franco Gorlero, Roberto Gherzi, Paola Briata

Correspondence

roberto.gherzi@hsanmartino.it (R.G.), paola.briata@hsanmartino.it (P.B.)

In Brief

Puppo et al. show that KHSRP, through influencing miR-192-5p maturation as well as alternative splicing of a cohort of pre-mRNAs, is crucial to maintaining the epithelial identity of mammary gland cells. TGF-β-induced KHSRP silencing causes gene expression changes that contribute to EMT.

Highlights

- miR-27b-3p is induced by TGF-β and silences KHSRP in mammary gland cells
- KHSRP silencing is required for TGF-β-induced EMT
- KHSRP promotes maturation of miR-192-5p that targets a group of EMT factors
- KHSRP controls alternative splicing of a set of pre-mRNAs to favor epithelial phenotype

Puppo et al., 2016, Cell Reports *16*, 967–978
July 26, 2016
http://dx.doi.org/10.1016/j.celrep.2016.06.055

Cell Reports
Article

OPEN ACCESS
CellPress

miRNA-Mediated KHSRP Silencing Rewires Distinct Post-transcriptional Programs during TGF-β-Induced Epithelial-to-Mesenchymal Transition

Margherita Puppo,[1,2,7] Gabriele Bucci,[3,7] Martina Rossi,[1,2] Matteo Giovarelli,[1,9] Domenico Bordo,[1] Arfa Moshiri,[1,6] Franco Gorlero,[4,5] Roberto Gherzi,[1,8,*] and Paola Briata[1,8,*]

[1]Gene Expression Regulation Laboratory, IRCCS AOU San Martino-IST, 16132 Genova, Italy
[2]DIMES Sezione Biochimica-Università di Genova, 16132 Genova, Italy
[3]Center for Translational Genomics and Bioinformatics, San Raffaele Scientific Institute, 20132 Milano, Italy
[4]S.C. Ginecologia e Ostetricia Galliera Hospital, 16128 Genova, Italy
[5]School of Medicine, DINOGMI, University of Genova, 16128 Genova, Italy
[6]Department of Biotechnology, School of Advanced Technologies in Medicine, Shahid Beheshti University of Medical Sciences, Tehran 198396-3113, Iran
[7]Co-first author
[8]Co-senior author
[9]Present address: Department of Biomedical and Clinical Sciences "Luigi Sacco," Università di Milano, 20157 Milano, Italy
*Correspondence: roberto.gherzi@hsanmartino.it (R.G.), paola.briata@hsanmartino.it (P.B.)
http://dx.doi.org/10.1016/j.celrep.2016.06.055

SUMMARY

Epithelial-to-mesenchymal transition (EMT) confers several traits to cancer cells that are required for malignant progression. Here, we report that miR-27b-3p-mediated silencing of the single-strand RNA binding protein KHSRP is required for transforming growth factor β (TGF-β)-induced EMT in mammary gland cells. Sustained KHSRP expression limits TGF-β-dependent induction of EMT factors and cell migration, whereas its knockdown in untreated cells mimics TGF-β-induced EMT. Genome-wide sequencing analyses revealed that KHSRP controls (1) levels of mature miR-192-5p, a microRNA that targets a group of EMT factors, and (2) alternative splicing of a cohort of pre-mRNAs related to cell adhesion and motility including *Cd44* and *Fgfr2*. KHSRP belongs to a ribonucleoprotein complex that includes hnRNPA1, and the two proteins cooperate in promoting epithelial-type exon usage of select pre-mRNAs. Thus, TGF-β-induced KHSRP silencing is central in a pathway leading to gene-expression changes that contribute to the cellular changes linked to EMT.

INTRODUCTION

Epithelial-to-mesenchymal transition (EMT) is a reversible transdifferentiation process in which epithelial cells lose their characteristics and instead acquire mesenchymal properties. EMT has been implicated in several physiological and pathological processes, including embryonic development, wound healing, organ fibrosis, and cancer progression (see Kalluri and Weinberg [2009] for a review).

Through EMT, cells gain the ability to migrate and resist apoptosis as well as the potential to enter stem cell-like states (De Craene and Berx, 2013; Ye and Weinberg, 2015). Phenotypical hallmarks of EMT include morphological changes from a cobblestone-like epithelial shape to a spindle-like fibroblast phenotype, loss of epithelial CDH1 (also known as E-cadherin) at cell junctions, and increased expression of mesenchymal CDH2 (also known as N-cadherin). The opposite transdifferentiation process, mesenchymal-to-epithelial transition (MET), is also possible (De Craene and Berx, 2013; Ye and Weinberg, 2015). For many years, it has been proposed that cancer cells undergo EMT to facilitate invasion and dissemination although recent evidence proposed that EMT is instead a prerequisite for acquisition of chemoresistance (Fischer et al., 2015; Zheng et al., 2015).

EMT is initiated by signals that cells receive from their microenvironment, and transforming growth factor β (TGF-β) is considered to act as a primary inducer of this process (Moustakas and Heldin, 2012; Katsuno et al., 2013). TGF-β belongs to a large family of structurally related factors, including activins and bone morphogenetic proteins (BMPs), which regulate cell growth, survival, differentiation, and migration (Shi and Massagué, 2003). TGF-β ligands signal through receptor serine/threonine kinases that, in turn, phosphorylate cell-specific SMAD proteins that form complexes with the common SMAD4, translocate into the nucleus and regulate gene expression by modulating gene transcription as well as by promoting maturation of select microRNAs (miRNAs) from precursors (Blahna and Hata, 2012).

Recently, we have demonstrated that the single-strand RNA-binding protein KHSRP (also known as KSRP) is a component of the TGF-β/BMP signaling pathway in multipotent C2C12 cells. TGF-β/BMP-activated SMAD proteins associate with KHSRP

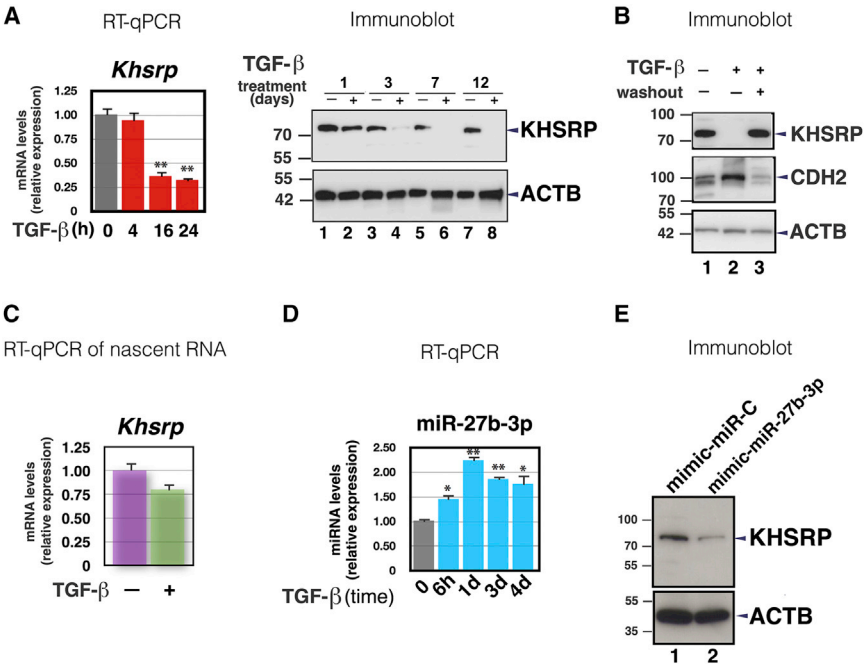

Figure 1. KHSRP Silencing during TGF-β-Induced EMT in NMuMg Cells

(A) Left: qRT-PCR analysis of *Khsrp* in NMuMg cells serum-starved (2% FBS, 16 hr) and either treated with TGF-β (10 ng/ml) for the indicated times or untreated (time 0). Right: immunoblot analysis of total cell extracts from NMuMg cells serum-starved and either treated with TGF-β (+) for the indicated times or untreated (–). The indicated antibodies were used.

(B) Immunoblot analysis of total cell extracts from NMuMg cells untreated (lane 1), treated with TGF-β for 7 days (lane 2), or treated with TGF-β for 7 days and then cultured in normal growth medium for 5 days (lane 3). The indicated antibodies were used.

(C) qRT-PCR analysis of nascent *Khsrp* transcript (Click-iT, see the Experimental Procedures) in NMuMg cells either untreated (–) or treated with TGF-β for 24 hr (+).

(D) qRT-PCR analysis of miR-27b-3p in NMuMg cells either untreated or treated with TGF-β for the indicated times.

(E) Immunoblot analysis of total cell extracts from either control- (mimic-miR-C) or mimic-miR-27b-3p- transfected NMuMg cells. The indicated antibodies were used.

The position of molecular mass markers is indicated on the left of each immunoblot. Representative gels are shown. The values of qRT-PCR experiments shown are averages ± SEM of three independent experiments performed in triplicate. Statistical significance: *$p < 0.01$, **$p < 0.001$ (Student's t test).

See also Figure S1.

and block its ability to promote maturation of myogenic miRNAs from precursors, thus orienting C2C12 cells toward osteoblastic differentiation. Accordingly, KHSRP silencing in C2C12 cells produces effects that largely coincide with those induced by TGF-β/BMP signaling activation (Pasero et al., 2012). Further, it has been recently reported that TGF-β regulates wound healing by controlling KHSRP levels and determining a switch between miR-198 and Follistatin-like 1 (FSTL1) protein expression (Sundaram et al., 2013). In general, KHSRP can be viewed as a multifunctional and versatile regulator of post-transcriptional switches that operates as a flexible effector of dynamic changes during transdifferentiation processes.

For these reasons, we decided to investigate KHSRP role in TGF-β-dependent EMT and provide evidence that miRNA-mediated KHSRP silencing is required for TGF-β-induced EMT in mammary gland cells. KHSRP is a crucial factor in maintaining the epithelial phenotype by promoting maturation of miR-192-5p from precursors and favoring the epithelial-type splicing pattern of a group of pre-mRNAs including *Cd44* and *Fgfr2*.

RESULTS

KHSRP Is Silenced during TGF-β-Induced Epithelial-to-Mesenchymal Transition in Mammary Gland Cells

In order to investigate whether KHSRP is implicated in TGF-β-induced EMT, we adopted the murine immortalized mammary epithelial cell line NMuMg as a model. These cells acquire mesenchymal traits and display the gene expression pattern typical of EMT in response to TGF-β (Avery-Cooper et al. [2014] and references cited therein) (Figures S1A–S1C). Importantly, KHSRP expression was silenced in a time-dependent manner in response to TGF-β (Figure 1A) and its levels were restored when TGF-β was removed from cultures (Figure 1B). qRT-PCR analysis of nascent transcripts showed that TGF-β produces a limited change in *Khsrp* transcription (Figure 1C) thus prompting us to investigate a post-transcriptional mechanism for TGF-β-dependent KHSRP silencing. Genome-wide deep RNA-sequencing (RNA-seq) analysis performed on the small RNA population (see below) revealed that two miRNAs (miR-27b-3p and miR-181a), previously reported to target KHSRP (Zhou et al., 2012; Sundaram et al., 2013), are induced by TGF-β in NMuMg cells with timing compatible with KHSRP downregulation (Figures 1D and S1D). miR-27b-3p transfection caused KHSRP downregulation in untreated NMuMg cells while miR-181a did not produce any effect (Figures 1E, S1E, and S1F). Furthermore, miR-27b-3p silencing prevented TGF-β-induced *Khsrp* downregulation (Figure S1G).

The observation that TGF-β causes KHSRP silencing was extended to other mammary epithelial cell lines known to undergo EMT in response to the cytokine treatment (human non-tumorigenic MCF 10A and human mammary epithelial (HMLE) cells as well as murine Py2T cells, Figure S1H). Conversely, TGF-β did not reduce KHSRP expression in breast cancer cell lines that display a limited EMT response to TGF-β such as MDA-MB-231, 4T1, TS/A, HMLER, and MCF7 (Figure S1I; data not shown).

Altogether, these results indicate that KHSRP is silenced by miR-27b-3p in mammary gland cell lines that undergo EMT in response to TGF-β.

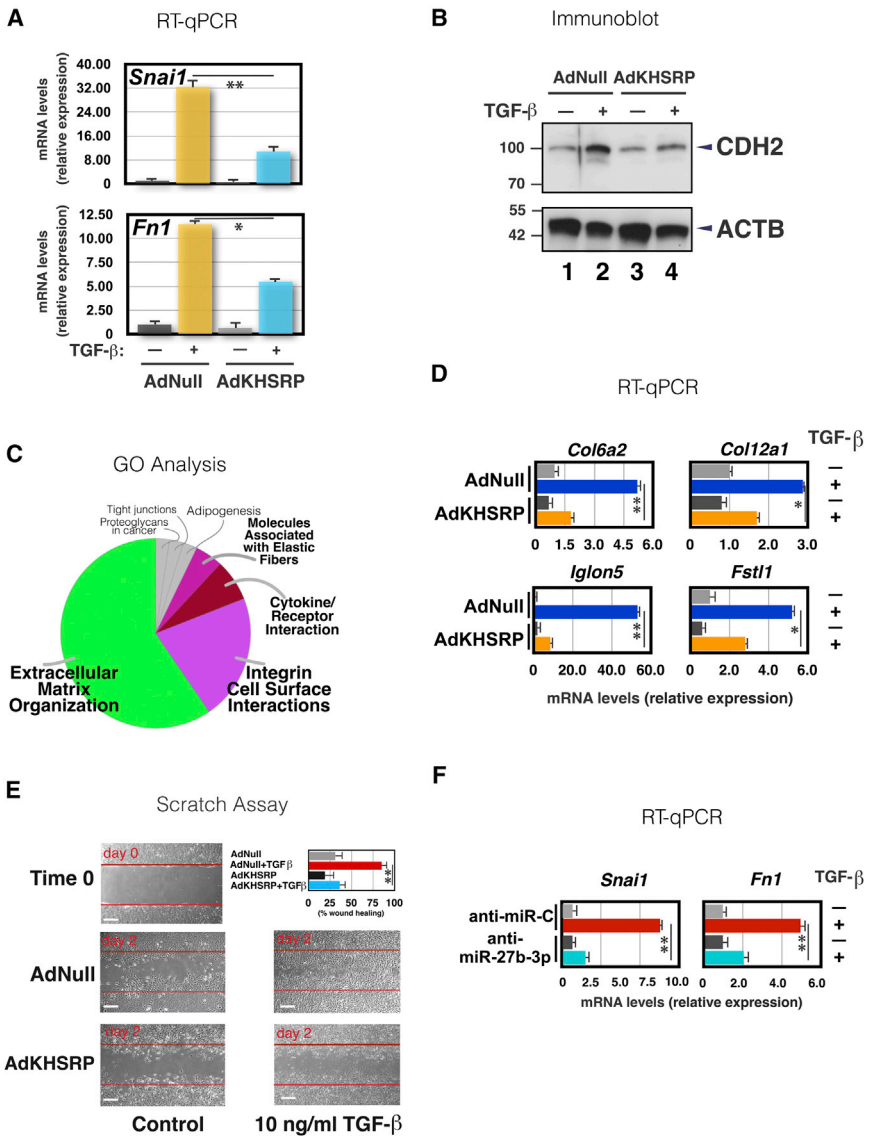

Figure 2. Forced KHSRP Expression Prevents TGF-β-Induced EMT and Reprograms the Transcriptome of NMuMg Cells

(A) qRT-PCR analysis of the indicated transcripts in NMuMg cells infected with either control (AdNull) or KHSRP-expressing (AdKHSRP) adenoviral vectors for 24 hr and subsequently serum-starved and either treated with TGF-β (+) for 24 hr or untreated (–).

(B) Immunoblot analysis of total cell extracts from cells treated as in (A). The indicated antibodies were used. The position of molecular mass markers is indicated on the left. Representative gels are shown.

(C) Gene Ontology (GO) analysis. RNA isolated from either AdNull- or AdKHSRP-expressing and TGF-β-treated NMuMg cells was subjected to RNA-seq analysis. Genes showing a log2-fold change >1.5 in the biological triplicates were used for GO analysis, and the enrichment of the KHSRP-regulated pathways are presented as pie graph.

(D) qRT-PCR analysis of the indicated transcripts in cells treated as in (A).

(E) Scratch wound healing assay. NMuMg cells were cultured as in (A) and scratch wounds were introduced into confluent monolayers. Cultures were photographed and the width of the wound was measured at 0 hr and 48 hr after the scratch was made. The percentage of the wound healed area for each culture condition was plotted (top right bar graph). Representative images are shown. Scale bars represent 100 μm.

(F) qRT-PCR analysis of the indicated transcripts in NMuMg cells transfected with either control anti-miRNA (anti-miR-C) or anti-miR-27b-3p and subsequently serum-starved and either treated with TGF-β (+) for 36 hr or untreated (–).

The values of qRT-PCR experiments shown are averages (±SEM) of three independent experiments performed in triplicate. Statistical significance: *$p < 0.005$, **$p < 0.001$ (Student's t test). See also Figure S2 and Table S1.

Forced KHSRP Expression Prevents TGF-β-Induced EMT and Reprograms the Transcriptome of NMuMg Cells

We investigated whether KHSRP downregulation is required for TGF-β-induced EMT. To this purpose, we transiently overexpressed KHSRP (AdKHSRP) in NMuMg cells—in order to maintain its constant levels during TGF-β treatment—and analyzed the expression of some factors known as hallmarks of EMT induction (Figure S2A). As shown in Figures 2A and 2B, KHSRP overexpression significantly impaired the TGF-β-dependent induction of *Snai1*, *Fn1* (a.k.a. fibronectin), and CDH2 (a.k.a. N-cadherin) when compared to control (AdNull) cells. Next, we performed RNA-seq analyses to investigate the changes induced in the whole transcriptome by sustained KHSRP expression. Gene Ontology enrichment (GO) analysis revealed that KHSRP-regulated transcripts were involved in cell adhesion, cell motility/migration, and cytokine/receptor interaction (Figure 2C). Our qRT-PCR-based validation of RNA-seq data showed that KHSRP overexpression counteracts the TGF-β-dependent induction of transcripts relevant to collagen metabolism (e.g., *Col12a1*, *Col6a2*), cell adhesion (e.g., *Iglon5*), TGF-β signaling (e.g., *Fstl1*), extracellular matrix organization (e.g., *Adamtsl2*, *Gpc6*, *Wisp2*), cytokine-receptor interaction (*Ccl17*), and glycosaminoglycan metabolism (e.g., *Chst1*) (Figures 2D and S2B; Table S1). Consistently, scratch wound assays revealed that KHSRP overexpression in TGF-β-treated cells reduces the wound closure when compared to negative control cells (Figure 2E). Finally, miR-27b-3p downregulation—similar to KHSRP overexpression—prevented TGF-β-dependent induction of *Snai1*, *Fn1*, *Cdh2*, *Zeb1*, and *Zeb2* gene expression (Figures 2F and S2C; Table S1).

Together, our results indicate that KHSRP-sustained expression impairs the TGF-β-dependent induction of factors related to cell adhesion and motility and suggests that TGF-β-induced

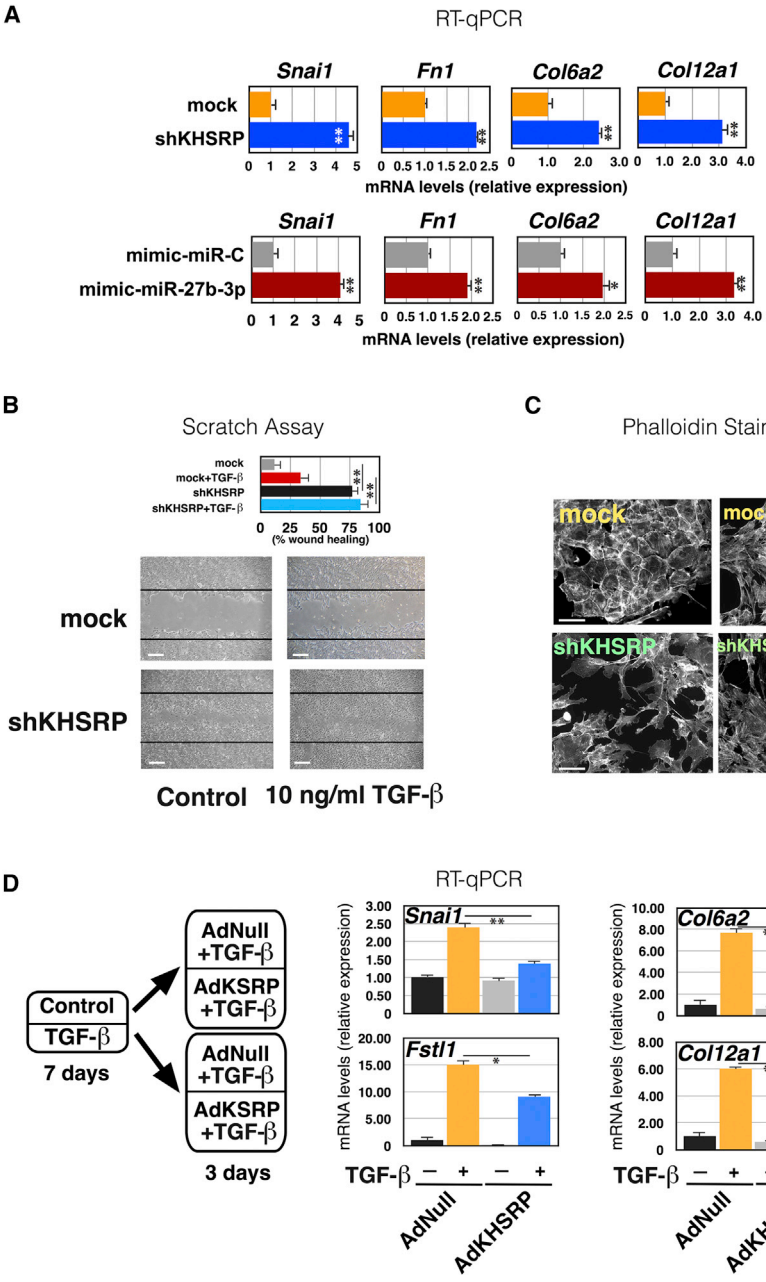

Figure 3. KHSRP Knockdown Mimics the Phenotype of TGF-β-Induced EMT

(A) qRT-PCR analysis of the indicated transcripts in either mock or shKHSRP untreated NMuMg cells (upper panels) and in either control miRNA mimic (mimic-miR-C) or mimic-miR-27b-3p (lower panels)-transfected NMuMg cells.

(B) Scratch wound healing assay. Either mock or shKHSRP NMuMg cells were serum-starved and then either treated with TGF-β or untreated. Scratch wounds were introduced into confluent monolayers. Cultures were photographed and the width of the wound was measured at 48 hr after the scratch was made. The percentage of the wound healed area for each culture condition was plotted (top right bar graph). Representative images are shown. Scale bars represent 100 μm.

(C) Either mock or shKHSRP NMuMg cells were serum-starved and then either treated with TGF-β or untreated for 48 hr. Cells were stained using Alexa Fluor 568 Phalloidin to visualize the actin cytoskeleton. Representative images are shown. Scale bars represent 50 μm.

(D) Left: schematic of the NMuMg cell treatment. Right: qRT-PCR analysis of the indicated transcripts in cells treated as summarized in the left panel.

The values of qRT-PCR experiments shown are averages ± SEM of three independent experiments performed in triplicate. Statistical significance: *$p < 0.01$, **$p < 0.001$ (Student's t test). See also Figure S3 and Table S1.

KHSRP silencing is required to enable NMuMg cells to acquire migratory properties.

KHSRP Knockdown Mimics the Phenotype of TGF-β-Induced EMT

In order to unambiguously establish the role of KHSRP silencing as a key step in TGF-β-induced EMT, we stably knocked-down KHSRP (shKHSRP) in NMuMg cells (Figure S3A) and found that shKHSRP mimics the effect of TGF-β on the expression of EMT-related factors (Figures 3A, top panels, and S3B; Table S1). Further, Figure 3A (bottom panels) and Table S1 show that forced miR-27b-3p expression, similar to KHSRP knockdown, induced expression of critical EMT factors.

Scratch wound assays showed that KHSRP knockdown accelerates the wound closure in both control and TGF-β-treated cells (Figure 3B), and the enhanced migratory potential of shKHSRP cells was confirmed by transwell migration assays (Figure S3C). According to a recent report (Yao et al., 2016), transient miR-27b-3p overexpression in NMuMg cells caused the appearance of increased migration areas in scratch wound assays (Figure S3D). KHSRP downregulation also mimicked the TGF-β-mediated remodeling of the cytoskeleton from cortical actin to stress fibers as determined by phalloidin staining (Figure 3C). Stable KHSRP knockdown mimicked the changes induced by TGF-β also in Py2T cells (Figures S3E and S3F; data not shown). Consistently, KHSRP overexpression impaired the wound healing in Py2T cells while its downregulation enhanced the gap closure (Figure S3G; data not shown).

Transient KHSRP re-expression reverted the EMT-like phenotype of shKHSRP NMuMg cells (Figures S3H and S3I). Most importantly, we showed that cells that achieved an established mesenchymal phenotype through a prolonged treatment with TGF-β reacquire an epithelial phenotype upon KHSRP

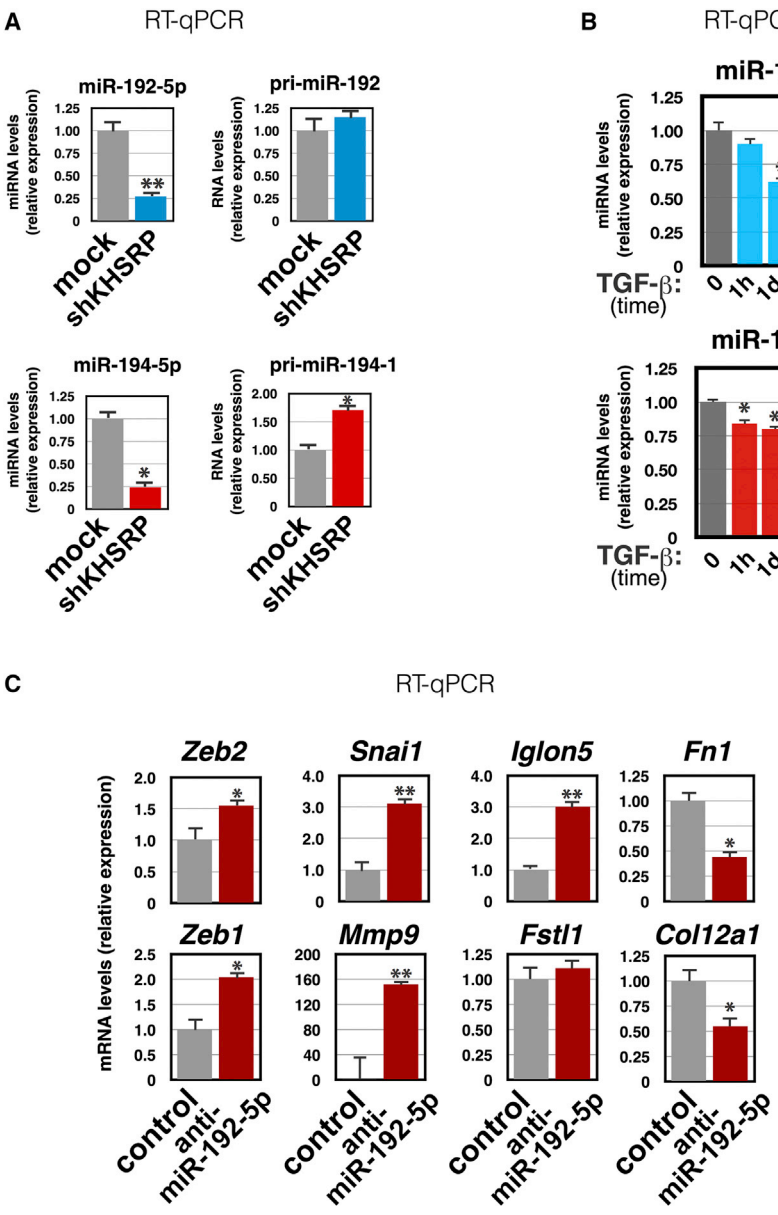

Figure 4. KHSRP-Dependent Maturation of miR-192-5p Prevents the Expression of Some EMT Factors

(A) qRT-PCR analysis of the indicated miRNAs or their primary transcripts in either mock or shKHSRP NMuMg cells.

(B) qRT-PCR analysis of the indicated miRNAs in serum-starved NMuMg cells either untreated or treated with TGF-β for the indicated times.

(C) qRT-PCR analysis of the indicated transcripts in NMuMg cells transfected with either miRNA inhibitor negative control or with miRCURY LNA miR-192-5p inhibitor.

The values of qRT-PCR experiments shown are averages ± SEM of three independent experiments performed in triplicate. Statistical significance: *$p < 0.01$, **$p < 0.001$ (Student's t test). See also Figure S4 and Table S1.

re-expression and despite the continuous presence of TGF-β (Figure 3D).

As a whole, these data indicate that KHSRP knockdown in untreated cells induces phenotypic changes that mimic TGF-β-induced EMT thus supporting our hypothesis that KHSRP silencing is a required event for EMT occurring in response to TGF-β.

KHSRP-Dependent Maturation of miR-192-5p Prevents the Expression of Some EMT Factors

Cellular and animal experimental models have demonstrated that KHSRP favors mRNA decay and miRNA maturation in an integrated way (reviewed in Briata et al., 2016). Here, we found that KHSRP is almost exclusively located in the nucleus of mammary gland cells (Figures S4A and S4B; data not shown). In agreement with this observation, KHSRP silencing did not affect the decay rate of several mRNAs whose expression was significantly increased upon either TGF-β-induced EMT or KHSRP silencing (Figure S4C; data not shown).

To explore the role of KHSRP in TGF-β-controlled miRNA maturation, we performed miRNA deep-sequencing analyses in shKHSRP NMuMg cells as well as in control mock-transfected cells. Bioinformatic analysis revealed that KHSRP knockdown significantly reduces the expression of a limited number of miRNAs (33 with p value $<10^{-3}$ using ANOVA test). qRT-PCR analysis revealed that KHSRP knockdown reduces the expression of miR-192-5p and miR-194-5p without affecting the levels of the corresponding primary transcripts and this indicates that KHSRP is required for the maturation of these miRNAs (Figures 4A and S4D; data not shown). Interestingly, the levels of miR-192-5p and miR-194-5p were downregulated in the course of TGF-β-induced EMT (Figure 4B). These observations, and the evidence that the expression of miR-192-5p and miR-194-5p inversely correlates with the metastatic potential of different cancer cells (Kim et al., 2011; Geng et al., 2014; Dong et al., 2011; Le et al., 2012), prompted us to investigate whether miR-192-5p and miR-194-5p silencing recapitulates gene expression changes induced by KHSRP silencing. Expression of anti-miR-192-5p in NMuMg cells upregulated *Zeb1*, *Zeb2*, as well as *Snai1*, *Iglon5*, and *Mmp9* expression while it did not affect *Fstl1* mRNA levels and even caused downregulation of *Fn1*, *Col6a2*, and *Col12a1* (Figure 4C; Table S1). Conversely, expression of anti-miR-194-5p did not affect the expression of EMT factors whose levels are regulated by KHSRP knockdown with the exception of a moderate increase in *Mmp9* expression (Figure S4E; Table S1).

In addition, the simultaneous silencing of the two miRNAs produced gene expression changes overlapping those caused by miR-192-5p silencing (data not shown).

In conclusion, because miR-192-5p and miR-194-5p silencing failed to reproduce the whole spectrum of gene expression changes induced by KHSRP downregulation, we hypothesized that KHSRP silencing during TGF-β-induced EMT impacts on an additional layer of post-transcriptional gene regulation.

KHSRP Controls Alternative Splicing of a Cohort of Pre-mRNAs Involved in Cell Adhesion and Migration

To investigate whether KHSRP affects pre-mRNA splicing in NMuMg cells, we applied a sensitive bioinformatic approach to detect genes subject to differential exon usage (DEXSeq) (Anders et al., 2012). In our RNA-seq data, we identified 763 alternative splicing events (log2 fold changes (FC) > |1.2|, BH (Bonferroni-corected, two-sided hypergeometric test) adjusted p value (adj.pval) < 0.01) involving 518 unique Ensembl transcripts that were controlled by KHSRP overexpression (Table S2). Among the regulated single cassette exons, 412 were less included while 351 were more included upon KHSRP overexpression, a ratio similar to that recently reported for other RNA binding proteins (RBPs) in a genome-wide analysis of alternative splicing (Huelga et al., 2012). Our findings are in line with recent evidence suggesting that modulation of alternative mRNA splicing plays a causative role in EMT (Cieply and Carstens, 2015) and with the original observation from the Black laboratory that KHSRP participates in alternative splicing (Min et al., 1997). GO enrichment analysis revealed that mRNAs whose splicing is affected by KHSRP overexpression are involved in biological processes such as cytoskeleton organization, cell junction assembly, and regulation of small GTPase-mediated signal transduction (Figure S5A).

Among these transcripts, we validated some of the KHSRP-controlled cassettes utilizing exon-specific primers by qRT-PCR and focused exclusively on exons that have been proven to generate alternative protein isoforms (according to the Ensembl annotation GRCm38.74; http://www.ensembl.org/). Figures 5A and S5B show some representative examples, including *Enah*, whose alternative splicing has been previously implicated in EMT (Warzecha et al., 2009).

Interestingly, ribonucleoprotein immunoprecipitation (RIP) analysis followed by RNA deep-sequencing performed in NMuMg cells (P.B. and R.G, unpublished data) revealed that KHSRP interacts with a number of pre-mRNAs including those encoding CD44 and FGFR2 (Warzecha et al., 2009; Brown et al., 2011) (Figure S5C; data not shown). It has been previously demonstrated that TGF-β treatment induces a shift from the epithelial forms of CD44 and FGFR2 (CD44v and FGFR2 IIIb, respectively) to the mesenchymal-specific forms (CD44s and FGFR2 IIIc, respectively) that are known to play a causative role in EMT (Warzecha et al., 2009; Brown et al., 2011; Cieply and Carstens, 2015). Although the log2 fold expression changes in the levels of the alternatively spliced *Cd44* and *Fgfr2* cassettes in our differential exon usage analysis of RNA-seq experiments did not reach the stringent cutoff value that we initially established, their expression changes were statistically relevant (p.adj < 0.01). Figure 5B shows that KHSRP overexpression significantly reduced the ratio between the mesenchymal-type *Cd44s* and the epithelial-type *Cd44v* isoform (*Cd44s/Cd44v*). Conversely, KHSRP knockdown significantly enhanced the *Cd44s/Cd44v* ratio mimicking TGF-β effect (Figure 5B). Similarly, KHSRP overexpression favored the inclusion of the *Fgfr2* epithelial-specific exon (*IIIb*), whereas KHSRP silencing favored the inclusion of the mesenchymal cassette (*IIIc*) in *Fgfr2* mRNA (Figure 5C). Figure S5D shows that KHSRP silencing induced a similar splicing pattern also in Py2T cells. Furthermore, we showed that KHSRP re-expression in NMuMg cells that achieved an established mesenchymal phenotype through a prolonged treatment with TGF-β (see Figures 3D and S3H) reverts the TGF-β-induced mesenchymal pattern of *Cd44* splicing (Figure S5E). miR-27b-3p overexpression in untreated NMuMg cells mimicked both TGF-β effect and KHSRP silencing by favoring mesenchymal-type splicing pattern of Cd44 pre-mRNA (Figure S5F, left). Conversely, miR-27b-3p silencing prevented in part the TGF-β-mediated exclusion of variable *Cd44* exons (Figure S5F, right).

In order to identify the *Enah*, *Cd44*, and *Fgfr2* pre-mRNA regions bound by KHSRP, we probed anti-KHSRP RIP experiments using intron-specific primers. A prominent KHSRP interaction with *Enah* intron 5-6, *Cd44* intron 8-9, and *Fgfr2* intron 5-6 was observed (Figure 5D; data not shown). The Cd44 region spanning i8-9 includes a consensus binding motif for KHSRP (identified on the basis of HITS-CLIP experiments) (D.B., G.B. P.B., and R.G., unpublished data), and we proved the direct interaction of recombinant KHSRP with this region by electrophoretic mobility shift assay (EMSA) (Figure S5G).

In order to support a direct regulation of CD44 alternative splicing by KHSRP, we transiently expressed a minigene splicing reporter construct including CD44 exon v8 and its flanking introns in HEK293 cells. Figure S5H shows that KHSRP interacts with the minigene in RIP experiments, and KHSRP knockdown favored exon v8 skipping as evaluated by qRT-PCR using specific primer sets that amplify exon CD44v8-included and CD44v8-skipped products.

Altogether, our results indicate that KHSRP influences the alternative splicing of a group of pre-mRNAs encoding factors involved in cell-cell and cell-matrix interactions as well as in cell migration.

KHSRP and hnRNPA1 Cooperate to Maintain the Epithelial-type Pre-mRNA Splicing Pattern of *Enah*, *Cd44*, and *Fgfr2*

Ribonucleoprotein complexes involving multiple regulatory RBPs able to modulate alternative splicing have recently emerged (see Aparicio et al. [2013], Fu and Ares [2014], and Cieply and Carstens [2015] for recent reviews).

We wanted to explore whether KHSRP associates with other RBPs that are able to control alternative splicing events in EMT. Epithelial splicing regulatory proteins 1 and 2 (ESRP1 and ESRP2, collectively indicated as ESRPs) are critical coordinators of an epithelial cell-type-specific splicing program in different cellular contexts (Warzecha et al., 2009; Bebee et al., 2015). Indeed, KHSRP co-immunoprecipitates with ESRPs and the proteins share similar pre-mRNA targets in 4T1 mammary gland cells (Figures S6A and S6B; data not shown). However, in NMuMg cells ESRP1 is not expressed while ESRP2 protein

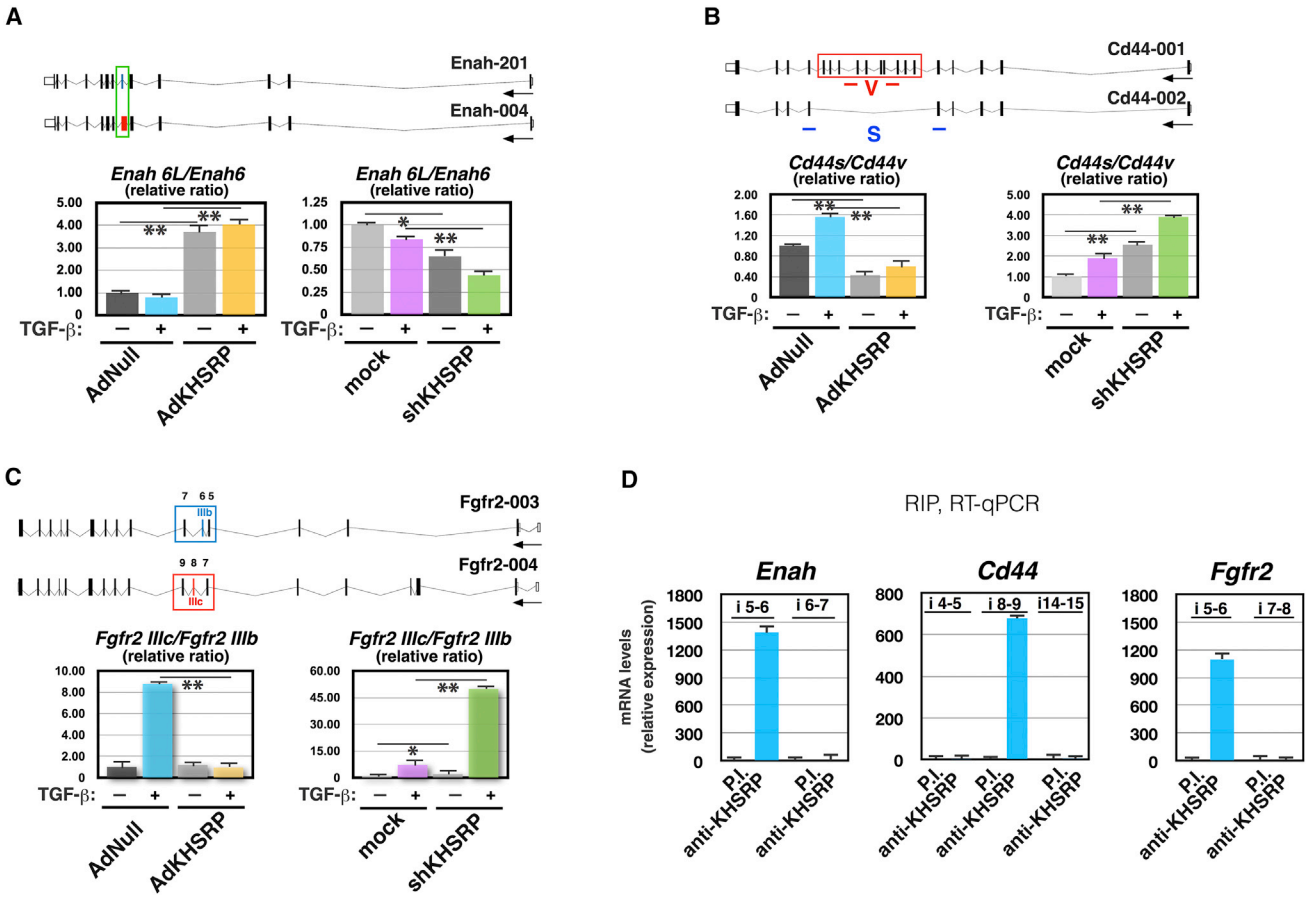

Figure 5. KHSRP Controls Alternative Splicing of *Enah*, *Cd44*, and *Fgfr2* Pre-mRNAs in NMuMg Cells

(A) Top: schematic of the exon-intron structure (not in scale) of *Enah* mRNA splice variants 201 and 004 (ENSMUSG00000022995). The green open box marks the alternatively spliced exons 6 and 6L (in red), respectively. Bottom: qRT-PCR analysis performed using exon-specific primers. The results are presented as ratio between the expression levels of *Enah* exon 6L-including and exon 6-including mRNA isoforms. NMuMg cells were infected with either control (AdNull) or KHSRP-expressing adenoviral vectors (AdKHSRP) for 24 hr and subsequently serum-starved and either treated with TGF-β (+) for 24 hr or untreated (–) (left). Either mock or shKHSRP NMuMg cells were serum-starved and then either treated with TGF-β or untreated for 24 hr (right).

(B) Top: schematic of the exon-intron structure (not in scale) of *Cd44* mRNA splice variants 001 and 002 (ENSMUSG00000005087). The red open box marks the alternatively spliced variable exons. The bars mark the position of primers used to detect, by qRT-PCR, the expression levels of variable (V) and standard (S) exons. Bottom: qRT-PCR analysis performed using the indicated primers. The results are presented as ratio between the expression levels of *Cd44s* and *Cd44v* mRNA isoforms. NMuMg cells were cultured as described in (A).

(C) Top: schematic of the exon-intron structure (not in scale) of *Fgfr2* mRNA splice variants 003 and 004 (ENSMUSG00000030849). The light blue and red open boxes mark the region including exons *IIIb* (exon 6 in *Fgfr2*-003) and *IIIc* (exon 8 in *Fgfr2*-004), respectively. Bottom: qRT-PCR analysis performed using exon-specific primers. The results are presented as ratio between the expression levels of exon *IIIc*- and exon *IIIb*- including mRNA isoforms. NMuMg cells were cultured as described in (A). Arrows in the schematics indicate the transcription direction.

(D) Total extracts from NMuMg cells were immunoprecipitated as indicated. RNA was purified from immunocomplexes and analyzed by qRT-PCR to detect the indicated pre-mRNAs.

The values of qRT-PCR experiments shown are averages ± SEM of three independent experiments performed in triplicate. Statistical significance: *$p < 0.01$, **$p < 0.001$ (Student's t test). See also Figure S5.

is expressed at low levels and does not interact with KHSRP (Figure 6B). Therefore, we explored the possibility that KHSRP may associate with a different ribonucleoprotein complex in NMuMg cells.

Some RBPs that have been implicated in splicing regulation during EMT are either not expressed or do not interact with KHSRP in NMuMg cells (data not shown; see the Discussion below). The multifunctional RBP hnRNPA1 has been recently implicated in cell-type-specific pre-mRNA splicing events (Bonomi et al., 2013; Douablin et al., 2015) and, interestingly, whereas the expression of KHSRP and other alternative splicing regulators is progressively silenced during EMT in NMuMg cells, the levels of hnRNPA1 remain constant during cell exposure to TGF-β (Figure 6A; data not shown). Co-immunoprecipitation experiments revealed that KHSRP associates with hnRNPA1 and that this interaction is abrogated by RNase A treatment (Figure 6B). This observation prompted us to explore whether KHSRP and hnRNPA1 interact with the same pre-mRNA regions

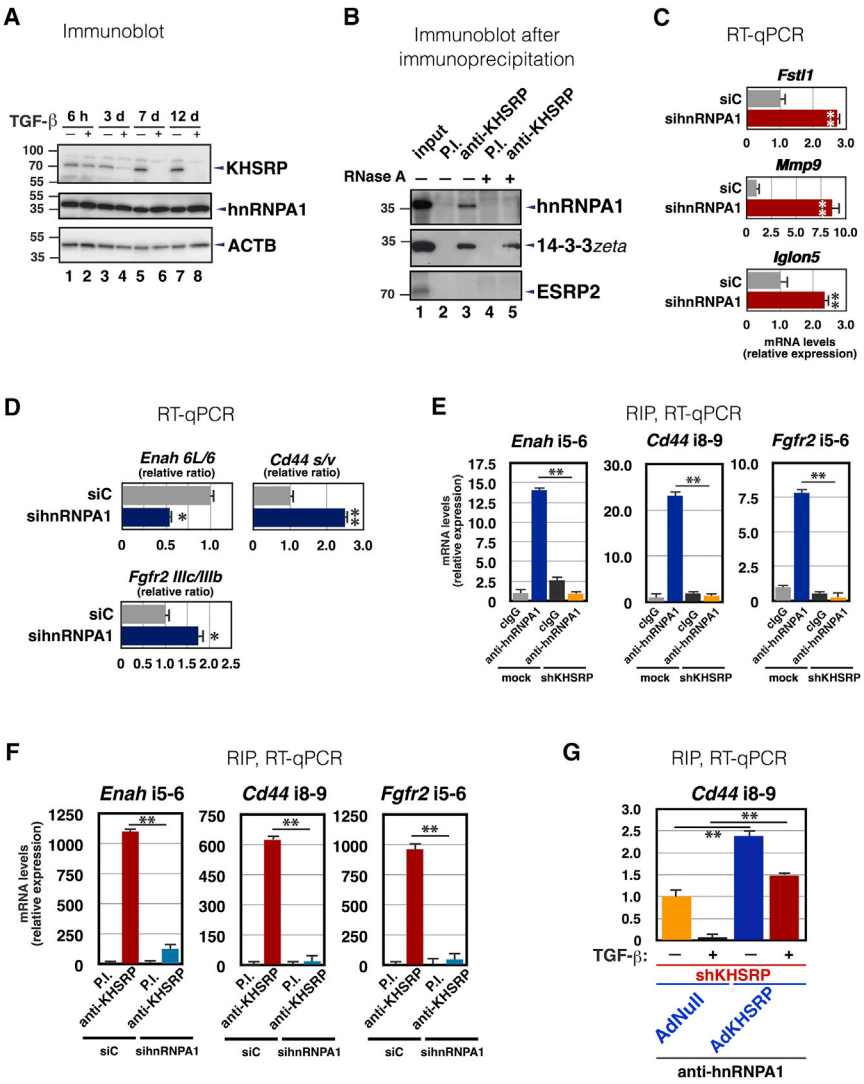

Figure 6. KHSRP and hnRNPA1 Cooperate to Maintain the Epithelial-type Pre-mRNA Splicing Pattern of *Enah*, *Cd44*, and *Fgfr2*

(A) Immunoblot analysis of total cell extracts from NMuMg cells serum-starved and either treated with TGF-β (+) for the indicated times or untreated (−). The indicated antibodies were used.

(B) Co-immunoprecipitation of hnRNPA1 and KHSRP in total extracts from NMuMg cells. Cell lysates either control-treated or treated with RNase A (10 μg/ml for 30 min at 37°C) were immunoprecipitated as indicated and analyzed by immunoblotting using the indicated antibodies.

(C) qRT-PCR analysis of the indicated transcripts in either control siRNA (siC) or sihnRNPA1-transfected NMuMg cells.

(D) qRT-PCR analysis performed using primers specific for the two isoforms of *Enah*, *Cd44*, and *Fgfr2* mRNAs, respectively. The results are presented as ratio between the expression levels of the indicated mRNA isoforms. NMuMg cells were transfected with either siC or sihnRNPA1 and collected 48 hr after transfection.

(E) Total extracts from either mock or shKHSRP NMuMg cells were immunoprecipitated as indicated. RNA was purified from immunocomplexes and analyzed by qRT-PCR to detect the indicated transcripts.

(F) Total extracts from NMuMg cells transfected with either siC or sihnRNPA1 were immunoprecipitated as indicated. RNA was purified from immunocomplexes and analyzed by qRT-PCR to detect the indicated transcripts.

(G) Total extracts from shKHSRP NMuMg cells, infected with either control (AdNull) or KHSRP-expressing (AdKHSRP) adenoviral vectors for 24 hr and subsequently serum-starved and either treated with TGF-β (+) for 24 hr or untreated (−), were immunoprecipitated as indicated. RNA was purified from immunocomplexes and analyzed by qRT-PCR to detect the indicated transcript.

The position of molecular mass markers is indicated on the left of each immunoblot. Representative gels are shown. The values of qRT-PCR experiments shown are averages ± SEM of three independent experiments performed in triplicate. Statistical significance: *$p < 0.01$, **$p < 0.001$ (Student's t test). See also Figure S6 and Table S1.

of *Enah*, *Cd44*, and *Fgfr2*. RIP analysis results presented in Figure S6C indicate that this is the case. Further, EMSA experiments revealed that recombinant hnRNPA1 directly interacts with *Cd44* (intron 8-9), the same region bound by recombinant KHSRP (Figure S6D).

In order to investigate a possible role of hnRNPA1 in TGF-β-dependent EMT, we transiently silenced hnRNPA1 in untreated NMuMg cells (Figure S6E) and found that its knockdown enhances the expression of a subset of EMT factors (Figure 6C; Table S1), whereas it does not affect miR-192-5p and miR-194-5p expression (Figure S6F). Further, data presented in Figure 6D shows that hnRNPA1 knockdown, similar to KHSRP silencing, promoted the mesenchymal-type exon usage of *Enah*, *Cd44*, and *Fgfr2* pre-mRNA.

The interaction of hnRNPA1 with *Enah*, *Cd44*, and *Fgfr2* pre-mRNAs is largely impaired by TGF-β treatment although the protein continues to be expressed (see Figures 6A and S6G; data not shown). Based on these findings, we investigated whether KHSRP and hnRNPA1 mutually influence their binding activity to *Enah*, *Cd44*, and *Fgfr2* and pre-mRNAs. Although either recombinant protein is able to bind a common target RNA in vitro (Figures S5G and S6D), RIP analyses shown in Figures 6E and 6F indicate that the ability of hnRNPA1 to interact with *Enah*, *Cd44*, and *Fgfr2* pre-mRNAs is significantly impaired by KHSRP knockdown, whereas the interaction of KHSRP with the same pre-mRNAs is strongly reduced in hnRNPA1-knockdown NMuMg cells. Finally, we showed that KHSRP re-expression in shKHSRP NMuMg cells was able to restore the ability of hnRNPA1 to interact with *Enah*, *Cd44*, and *Fgfr2* pre-mRNAs (Figure 6G; data not shown; see also Figure S3H).

As a whole, our results suggest that KHSRP and hnRNPA1 are mutually necessary for binding to *Enah*, *Cd44*, and *Fgfr2*

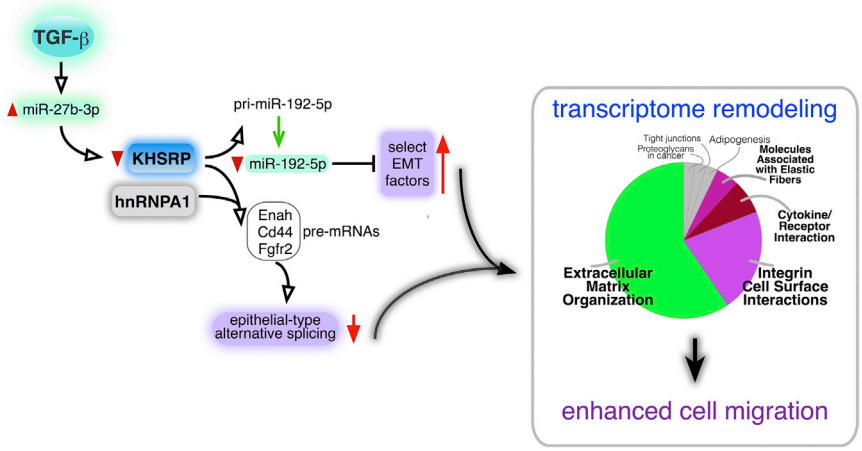

Figure 7. Schematic Model Summarizing the Mechanism by which TGF-β-Induced KHSRP Silencing Contributes to EMT in Mammary Gland NMuMg Cells

Black arrows indicate the steps of KHSRP-regulated pathway. Red arrows indicate up- or down-regulation of crucial events. The green arrow indicates the maturation pathway of primary miR-192 maturation.

pre-mRNAs and for maintaining the epithelial-type exon usage of these transcripts in NMuMg cells.

DISCUSSION

Here, we report that TGF-β-dependent early induction of miR-27b-3p silences KHSRP in non-transformed mammary gland cells. This produces a vast rearrangement of the transcriptome and contributes to EMT. KHSRP silencing impairs maturation of miR-192-5p, with the consequent upregulation of a subset of EMT factors, and favors alternative exon usage of genes involved in cell adhesion and migration (a schematic of the pathway is shown in Figure 7).

Our previous and current experiments suggest that ligands belonging to the TGF-β family need to overcome KHSRP function in order to orient cell differentiation decisions. This is achieved either through SMAD-mediated inhibition of KHSRP activity that leads to a maturation blockade of pro-myogenic miRNAs (Pasero et al., 2012) or through abrogation of KHSRP expression as in the case of the present study. Here, we report that miR-27b-3p is a component of the TGF-β signaling pathway that contributes to development of the EMT process through KHSRP silencing. A miRNA-mediated downregulation of KHSRP expression by TGF-β has also been reported by Sundaram et al. (2013) showing that miR-181a-dependent KHSRP silencing leads to a switch between primate-specific miR-198 maturation and FSTL1 protein expression during wound healing. The fact that in our model KHSRP silencing is achieved through a distinct miRNA and results in a different cascade of events put forward the idea that TGF-β family members operate in a variety of ways to silence KHSRP expression/function and emphasizes the importance of the "TGF-β/KHSRP antagonism" as a hub during TGF-β-family-member-driven cell differentiation.

Although TGF-β-dependent KHSRP silencing controls the expression of miRNAs previously implicated in EMT (Zhang et al., 2014; data not shown), we decided to analyze in detail the miR-192-5p function because its maturation from primary transcripts is directly controlled by KHSRP. However, the evidence that miR-192-5p silencing fails to reproduce the whole spectrum of gene expression changes caused by KHSRP silencing, prompted us to explore the impact of KHSRP on an additional layer of regulation.

Despite the fact that biochemical experiments uncovered KHSRP involvement in alternative splicing almost 20 years ago (Min et al., 1997), we now show the role of KHSRP-modulated exon usage in a cell transdifferentiation model. Regulation of gene expression by alternative splicing was the first posttranscriptional mechanism linked to EMT (Savagner et al., 1994) and, indeed, it can impact on all the events described as "hallmarks of cancer." RBPs able to control alternative splicing have emerged as critical regulators of EMT in the last few years. Huelga et al. (2012) demonstrated on a genomic scale that RBPs coordinately regulate hundreds of pre-mRNA alternative splicing events forming dynamically regulated complexes. Here, we report on the interaction between KHSRP and ESRPs in cells that co-express the three proteins. However, ESRP1 is not expressed while ESRP2 protein levels are low in NMuMg cells (data not shown). Similarly, Lin28, a factor recently reported as a modulator of alternative splicing in breast cancer cells (Yang et al., 2015), is not expressed in NMuMg cells (data not shown). RNA helicases DDX5 and DDX17 have been implicated at different transcriptional and posttranscriptional levels in EMT and their expression is silenced by TGF-β treatment (Dardenne et al., 2014). However, their knockdown failed to affect the expression of EMT factors and to influence the KHSRP-dependent alternative splicing events in NMuMg cells (P.B. and R.G., unpublished observation). Xu et al., (2014) have recently demonstrated that hnRNPM, competing with ESRP1, favors the mesenchymal-type alternative splicing of CD44 and other pre-mRNAs and promotes breast cancer metastasis by activating EMT. Also in this case, the fact that ESRP1 is absent and hnRNPM expression is silenced in a time-dependent manner in response to TGF-β in NMuMg cells (data not shown) makes it unlikely that this regulatory network is operative in our model. RBFOX2 is another important alternative splicing regulator in different tissues (Shapiro et al., 2011; Braeutigam et al., 2014, Damianov et al., 2016). However, a comparison of RBFOX2 target transcripts described elsewhere (Braeutigam et al., 2014) with the results of our analysis failed to reveal any overlap.

hnRNPA1 has been implicated in a number of cellular processes, including pre-mRNA splicing regulation (Matter et al., 2000; He and Smith, 2009; Bonomi et al., 2013; Douablin et al., 2015), and we and others have previously observed that KHSRP and hnRNPA1 associate in different cell types (Ruggiero

et al., 2007; Michlewski and Cáceres, 2010). Michlewski and Cáceres (2010) demonstrated that the two proteins show similar binding preferences to RNA sequences (Trabucchi et al., 2009), and our in vitro binding data indicate that KHSRP and hnRNPA1 directly bind to a region located in the intron 8-9 of *Cd44* pre-mRNA. Interestingly, this sequence includes two GGG triplets, a preferred binding site for both KHSRP (Trabucchi et al., 2009), and hnRNPA1 (Michlewski and Cáceres, 2010). On the basis of our RIP analyses, it is tempting to speculate that KHSRP and hnRNPA1 form a complex with *Enah*, *Cd44*, and *Fgfr2* pre-mRNAs, respectively, and each protein is required to allow the other to interact with these target transcripts. TGF-β-induced KHSRP downregulation causes a destabilization of the RNA-protein complex and hnRNPA1, although still present, is unable to interact with *Enah*, *Cd44*, and *Fgfr2* pre-mRNAs.

Two recent reports suggested a major role for EMT in chemoresistance, and the analysis of our RNA-seq data showed that KHSRP regulates the expression of a relevant number of transcripts involved in drug transport and metabolism (Fischer et al., 2015; Zheng et al., 2015) (Table S3). This allows us to hypothesize that, in addition to affecting cell adhesion and migration, KHSRP could influence the expression of factors relevant to other crucial EMT-driven events.

NMuMg cells used in our studies are representative of an early stage of mammary transformation and respond to TGF-β-inducing KHSRP silencing and, as a consequence, a variety of EMT-like phenotypic changes. In more advanced stages of transformation, cells become independent of TGF-β signaling and KHSRP silencing fails to occur. This is in agreement with the evidence that human tumors acquire loss-of-function mutations in the genes encoding TGF-β receptors or SMAD proteins (Pardali and Moustakas, 2007). We speculate that KHSRP silencing is required in early stages of transformation in order to enable TGF-β to initiate cell transdifferentiation process. Our contribution to the understanding of how TGF-β-modulated KHSRP expression affects distinct layers of posttranscriptional gene control provides insights in the biology of epithelial cells that are poised to undergo a transition toward a mesenchymal phenotype.

EXPERIMENTAL PROCEDURES

Cell Cultures and Treatments

Murine immortalized NMuMg cells (obtained from ATCC) were cultured in DMEM plus 10% FBS and 10 μg/ml bovine insulin (Sigma-Aldrich). HEK293 cells (obtained from ATCC) were cultured in DMEM plus 10% FBS. Py2T cells, a kind gift of Dr. G. Christofori (University of Basel), were cultured in DMEM plus 10% FBS as described (Waldmeier et al., 2012). The immortalized HMLE cells, a kind gift of Dr. R. Weinberg (Whitehead Institute), were cultured as described (Elenbaas et al., 2001). Human mammary gland adenocarcinoma cells MDA-MB-231 and MCF7 were cultured in DMEM plus 5% FBS; human non-tumorigenic epithelial cell line MCF 10A were cultured in DMEM/F12 plus 5% horse serum, 10 μg/ml bovine insulin (Sigma-Aldrich), EGF (20 ng/ml, Sigma-Aldrich), hydrocortisone (0.5 μg/ml, Sigma-Aldrich), and cholera toxin (100 ng/ml, Sigma-Aldrich). 4T1 and TS/A mouse mammary gland cancer cells (obtained from Dr. C. Bagni, VIB Center for the Biology of Disease) were cultured in DMEM/F12 plus 10% FBS.

NMuMg and Py2T cells were maintained in DMEM supplemented with 2% and 1% FBS, respectively, for 8–16 hr prior to the addition of 10 ng/ml human recombinant TGF-β1 purchased from R&D Systems.

Phalloidin Staining

Mock and shKHSRP NMuMg cells were fixed in 3.7% formaldehyde, stained using Alexa Fluor 568 Phalloidin, and imaged with the Imager M2 microscope (Zeiss).

Scratch Wound Closure Assay

Cells were cultured in six-well plates up to sub-confluence and maintained in 2% FBS-containing medium for 16 hr. After starvation, a wound was scratched into confluent monolayers, and cultures were either maintained in 2% FBS-containing medium for 48 hr or treated with 10 ng/ml TGF-β in the same medium for different times. Images were taken using a Olympus CKX41 microscope at different time post-wounding and analyzed using the ImageJ package (http://imagej.nih.gov/ij/index.html). Average distance of wound obtained from six microscopic fields was used for calculation of percent wound healed. Experiments were performed three times.

Exon-Level Quantification and Splicing Analysis

To test differences in exon usage, we followed the procedure described for DEXSeq (v 1.14.2, R 3.2.2) (Anders et al., 2012) adapting linear model design to test for differential usage induced by TGF-β in the presence or absence of KHSRP overexpression (cells infected with either AdKHSRP or AdNull, respectively). IN brief, we first created a GFF file from the Ensembl GRCm38.74 GTF with the provided script dexseq_prepare_annotation. Reads counts were then collected from the sorted_by_name BAM, with dexseq_count.py on the previously created GFF reference in "unstranded" "paired" mode. Exons with log2 fold change greater than |1.2| (linear FC 2.3), showing an adjusted p value <0.01 (FDR <1%, Benjamin-Hochberg corrected) were selected for downstream analysis.

ACCESSION NUMBERS

The accession numbers for the small RNA-seq and RNA-seq data reported in this article are NCBI SRA: SRP074885 and NCBI SRA: SRP070690, respectively.

SUPPLEMENTAL INFORMATION

Supplemental Information includes Supplemental Experimental Procedures, six figures, and four tables and can be found with this article online at http://dx.doi.org/10.1016/j.celrep.2016.06.055.

AUTHOR CONTRIBUTIONS

P.B. and R.G., conceived the experiments, wrote the manuscript, secured funding, supervised the experimental work, and conducted some experiments. M.P. and G.B., conducted the majority of the experiments and contributed to the editing of the manuscript. M.R. and M.G. performed some experiments. G.B. provided essential bioinformatics expertise. M.P., M.R., D.B., A.M., and F.G. provided discussion, feedback, and editorial support.

ACKNOWLEDGMENTS

We thank Drs. Bob Weinberg (Whitehead Institute), Gerhard Christofori (University of Basel), Chonghui Cheng (Northwestern University), Claudia Bagni (University of Leuven), and Gilberto Fronza (IRCCS San Martino-IST) for sharing cells and reagents. This project has been supported, in part, by grants from the Associazione Italiana per la Ricerca sul Cancro (AIRC I.G. grant 10090), the Association for International Cancer Research (AICR IG 2014 grant 15195) to R.G., and the Italian Ministero della Salute 5xmille 2013 to P.B.

Received: February 22, 2016
Revised: May 12, 2016
Accepted: June 12, 2016
Published: July 7, 2016

REFERENCES

Anders, S., Reyes, A., and Huber, W. (2012). Detecting differential usage of exons from RNA-seq data. Genome Res. *22*, 2008–2017.

Aparicio, L.A., Abella, V., Valladares, M., and Figueroa, A. (2013). Posttranscriptional regulation by RNA-binding proteins during epithelial-to-mesenchymal transition. Cell. Mol. Life Sci. *70*, 4463–4477.

Avery-Cooper, G., Doerr, M., Gilbert, R.W., Youssef, M., Richard, A., Huether, P., and Viloria-Petit, A.M. (2014). Par6 is an essential mediator of apoptotic response to transforming growth factor beta in NMuMG immortalized mammary cells. Cancer Cell Int. *14*, 19.

Bebee, T.W., Park, J.W., Sheridan, K.I., Warzecha, C.C., Cieply, B.W., Rohacek, A.M., Xing, Y., and Carstens, R.P. (2015). The splicing regulators Esrp1 and Esrp2 direct an epithelial splicing program essential for mammalian development. eLife *4*, e08954.

Blahna, M.T., and Hata, A. (2012). Smad-mediated regulation of microRNA biosynthesis. FEBS Lett. *586*, 1906–1912.

Bonomi, S., di Matteo, A., Buratti, E., Cabianca, D.S., Baralle, F.E., Ghigna, C., and Biamonti, G. (2013). HnRNP A1 controls a splicing regulatory circuit promoting mesenchymal-to-epithelial transition. Nucleic Acids Res. *41*, 8665–8679.

Braeutigam, C., Rago, L., Rolke, A., Waldmeier, L., Christofori, G., and Winter, J. (2014). The RNA-binding protein Rbfox2: an essential regulator of EMT-driven alternative splicing and a mediator of cellular invasion. Oncogene *33*, 1082–1092.

Briata, P., Bordo, D., Puppo, M., Gorlero, F., Rossi, M., Perrone-Bizzozero, N., and Gherzi, R. (2016). Diverse roles of the nucleic acid-binding protein KHSRP in cell differentiation and disease. Wiley Interdiscip. Rev. RNA *7*, 227–240.

Brown, R.L., Reinke, L.M., Damerow, M.S., Perez, D., Chodosh, L.A., Yang, J., and Cheng, C. (2011). CD44 splice isoform switching in human and mouse epithelium is essential for epithelial-mesenchymal transition and breast cancer progression. J. Clin. Invest. *121*, 1064–1074.

Cieply, B., and Carstens, R.P. (2015). Functional roles of alternative splicing factors in human disease. Wiley Interdiscip. Rev. RNA *6*, 311–326.

Damianov, A., Ying, Y., Lin, C.H., Lee, J.A., Tran, D., Vashisht, A.A., Bahrami-Samani, E., Xing, Y., Martin, K.C., Wohlschlegel, J.A., and Black, D.L. (2016). Rbfox proteins regulate splicing as part of a large multiprotein complex LASR. Cell *165*, 606–619.

Dardenne, E., Polay Espinoza, M., Fattet, L., Germann, S., Lambert, M.P., Neil, H., Zonta, E., Mortada, H., Gratadou, L., Deygas, M., et al. (2014). RNA helicases DDX5 and DDX17 dynamically orchestrate transcription, miRNA, and splicing programs in cell differentiation. Cell Rep. *7*, 1900–1913.

De Craene, B., and Berx, G. (2013). Regulatory networks defining EMT during cancer initiation and progression. Nat. Rev. Cancer *13*, 97–110.

Dong, P., Kaneuchi, M., Watari, H., Hamada, J., Sudo, S., Ju, J., and Sakuragi, N. (2011). MicroRNA-194 inhibits epithelial to mesenchymal transition of endometrial cancer cells by targeting oncogene BMI-1. Mol. Cancer *10*, 99.

Douablin, A., Deguillien, M., Breig, O., and Baklouti, F. (2015). HnRNP A1 tethers KSRP to an exon splicing silencer that inhibits an erythroid-specific splicing event in PU.1-induced erythroleukemia. Am. J. Cancer Res. *5*, 1410–1422.

Elenbaas, B., Spirio, L., Koerner, F., Fleming, M.D., Zimonjic, D.B., Donaher, J.L., Popescu, N.C., Hahn, W.C., and Weinberg, R.A. (2001). Human breast cancer cells generated by oncogenic transformation of primary mammary epithelial cells. Genes Dev. *15*, 50–65.

Fischer, K.R., Durrans, A., Lee, S., Sheng, J., Li, F., Wong, S.T., Choi, H., El Rayes, T., Ryu, S., Troeger, J., et al. (2015). Epithelial-to-mesenchymal transition is not required for lung metastasis but contributes to chemoresistance. Nature *527*, 472–476.

Fu, X.D., and Ares, M., Jr. (2014). Context-dependent control of alternative splicing by RNA-binding proteins. Nat. Rev. Genet. *15*, 689–701.

Geng, L., Chaudhuri, A., Talmon, G., Wisecarver, J.L., Are, C., Brattain, M., and Wang, J. (2014). MicroRNA-192 suppresses liver metastasis of colon cancer. Oncogene *33*, 5332–5340.

He, Y., and Smith, R. (2009). Nuclear functions of heterogeneous nuclear ribonucleoproteins A/B. Cell. Mol. Life Sci. *66*, 1239–1256.

Huelga, S.C., Vu, A.Q., Arnold, J.D., Liang, T.Y., Liu, P.P., Yan, B.Y., Donohue, J.P., Shiue, L., Hoon, S., Brenner, S., et al. (2012). Integrative genome-wide analysis reveals cooperative regulation of alternative splicing by hnRNP proteins. Cell Rep. *1*, 167–178.

Kalluri, R., and Weinberg, R.A. (2009). The basics of epithelial-mesenchymal transition. J. Clin. Invest. *119*, 1420–1428.

Katsuno, Y., Lamouille, S., and Derynck, R. (2013). TGF-β signaling and epithelial-mesenchymal transition in cancer progression. Curr. Opin. Oncol. *25*, 76–84.

Kim, T., Veronese, A., Pichiorri, F., Lee, T.J., Jeon, Y.J., Volinia, S., Pineau, P., Marchio, A., Palatini, J., Suh, S.S., et al. (2011). p53 regulates epithelial-mesenchymal transition through microRNAs targeting ZEB1 and ZEB2. J. Exp. Med. *208*, 875–883.

Le, X.F., Almeida, M.I., Mao, W., Spizzo, R., Rossi, S., Nicoloso, M.S., Zhang, S., Wu, Y., Calin, G.A., and Bast, R.C., Jr. (2012). Modulation of MicroRNA-194 and cell migration by HER2-targeting trastuzumab in breast cancer. PLoS ONE *7*, e41170.

Matter, N., Marx, M., Weg-Remers, S., Ponta, H., Herrlich, P., and König, H. (2000). Heterogeneous ribonucleoprotein A1 is part of an exon-specific splice-silencing complex controlled by oncogenic signaling pathways. J. Biol. Chem. *275*, 35353–35360.

Michlewski, G., and Cáceres, J.F. (2010). Antagonistic role of hnRNP A1 and KSRP in the regulation of let-7a biogenesis. Nat. Struct. Mol. Biol. *17*, 1011–1018.

Min, H., Turck, C.W., Nikolic, J.M., and Black, D.L. (1997). A new regulatory protein, KSRP, mediates exon inclusion through an intronic splicing enhancer. Genes Dev. *11*, 1023–1036.

Moustakas, A., and Heldin, C.-H. (2012). Induction of epithelial-mesenchymal transition by transforming growth factor β. Semin. Cancer Biol. *22*, 446–454.

Pardali, K., and Moustakas, A. (2007). Actions of TGF-beta as tumor suppressor and pro-metastatic factor in human cancer. Biochim. Biophys. Acta *1775*, 21–62.

Pasero, M., Giovarelli, M., Bucci, G., Gherzi, R., and Briata, P. (2012). Bone morphogenetic protein/SMAD signaling orients cell fate decision by impairing KSRP-dependent microRNA maturation. Cell Rep. *2*, 1159–1168.

Ruggiero, T., Trabucchi, M., Ponassi, M., Corte, G., Chen, C.Y., al-Haj, L., Khabar, K.S., Briata, P., and Gherzi, R. (2007). Identification of a set of KSRP target transcripts upregulated by PI3K-AKT signaling. BMC Mol. Biol. *8*, 28.

Savagner, P., Vallés, A.M., Jouanneau, J., Yamada, K.M., and Thiery, J.P. (1994). Alternative splicing in fibroblast growth factor receptor 2 is associated with induced epithelial-mesenchymal transition in rat bladder carcinoma cells. Mol. Biol. Cell *5*, 851–862.

Shapiro, I.M., Cheng, A.W., Flytzanis, N.C., Balsamo, M., Condeelis, J.S., Oktay, M.H., Burge, C.B., and Gertler, F.B. (2011). An EMT-driven alternative splicing program occurs in human breast cancer and modulates cellular phenotype. PLoS Genet. *7*, e1002218.

Shi, Y., and Massagué, J. (2003). Mechanisms of TGF-beta signaling from cell membrane to the nucleus. Cell *113*, 685–700.

Sundaram, G.M., Common, J.E., Gopal, F.E., Srikanta, S., Lakshman, K., Lunny, D.P., Lim, T.C., Tanavde, V., Lane, E.B., and Sampath, P. (2013). 'See-saw' expression of microRNA-198 and FSTL1 from a single transcript in wound healing. Nature *495*, 103–106.

Trabucchi, M., Briata, P., Garcia-Mayoral, M., Haase, A.D., Filipowicz, W., Ramos, A., Gherzi, R., and Rosenfeld, M.G. (2009). The RNA-binding protein KSRP promotes the biogenesis of a subset of microRNAs. Nature *459*, 1010–1014.

Waldmeier, L., Meyer-Schaller, N., Diepenbruck, M., and Christofori, G. (2012). Py2T murine breast cancer cells, a versatile model of TGFβ-induced EMT in vitro and in vivo. PLoS ONE *7*, e48651.

Warzecha, C.C., Sato, T.K., Nabet, B., Hogenesch, J.B., and Carstens, R.P. (2009). ESRP1 and ESRP2 are epithelial cell-type-specific regulators of FGFR2 splicing. Mol. Cell *33*, 591–601.

Xu, Y., Gao, X.D., Lee, J.H., Huang, H., Tan, H., Ahn, J., Reinke, L.M., Peter, M.E., Feng, Y., Gius, D., et al. (2014). Cell type-restricted activity of hnRNPM promotes breast cancer metastasis via regulating alternative splicing. Genes Dev. *28*, 1191–1203.

Yang, J., Bennett, B.D., Luo, S., Inoue, K., Grimm, S.A., Schroth, G.P., Bushel, P.R., Kinyamu, H.K., and Archer, T.K. (2015). LIN28A modulates splicing and gene expression programs in breast cancer cells. Mol. Cell. Biol. *35*, 3225–3243.

Yao, J., Deng, B., Zheng, L., Dou, L., Guo, Y., and Guo, K. (2016). miR-27b is upregulated in cervical carcinogenesis and promotes cell growth and invasion by regulating CDH11 and epithelial-mesenchymal transition. Oncol. Rep. *35*, 1645–1651.

Ye, X., and Weinberg, R.A. (2015). Epithelial-mesenchymal plasticity: a central regulator of cancer progression. Trends Cell Biol. *25*, 675–686.

Zhang, Y., Yang, P., and Wang, X.F. (2014). Microenvironmental regulation of cancer metastasis by miRNAs. Trends Cell Biol. *24*, 153–160.

Zheng, X., Carstens, J.L., Kim, J., Scheible, M., Kaye, J., Sugimoto, H., Wu, C.C., LeBleu, V.S., and Kalluri, R. (2015). Epithelial-to-mesenchymal transition is dispensable for metastasis but induces chemoresistance in pancreatic cancer. Nature *527*, 525–530.

Zhou, R., Gong, A.Y., Eischeid, A.N., and Chen, X.M. (2012). miR-27b targets KSRP to coordinate TLR4-mediated epithelial defense against Cryptosporidium parvum infection. PLoS Pathog. *8*, e1002702.